Colloid Polym Sci (2017) 295:327–340
DOI 10.1007/s00396-016-4006-4

ORIGINAL CONTRIBUTION

A thermo-sensitive OEGMA-based polymer: synthesis, characterization and interactions with surfactants in aqueous solutions with and without salt

Yi Guo[1] · Xiuyan Dong[1] · Wenjing Ruan[1] · Yazhuo Shang[1] · Honglai Liu[1]

Received: 12 May 2016 / Accepted: 12 December 2016 / Published online: 30 December 2016

Abstract The interactions between poly(2-(2-methoxyethoxy)ethyl methacrylate$_{90}$-co-oligo(ethylene glycol) methacrylate$_{10}$) (P(MEO_2MA_{90}-co-$OEGMA_{10}$)) and sodium dodecyl sulfate (SDS) or dodecyltrimethyl ammonium bromide (DTAB) in aqueous solutions with and without salt are explored. The influence rule of surfactant on thermo-sensitive behavior of polymer and the corresponding mechanism is revealed. The results have suggested that both surfactants have moderate interactions with P(MEO_2MA_{90}-co-$OEGMA_{10}$), which result in the formation of P(MEO_2MA_{90}-co-$OEGMA_{10}$)/surfactant complexes. Meanwhile, the self-aggregation of polymer chains is hindered causing the lower critical solution temperatures (LCSTs) increase due to the electrostatic repulsion and "locking water" effect caused by surfactant head groups. Tetra-n-butylammonium bromide (Bu_4NBr) and tetra-n-propylammonium bromide (Pr_4NBr) can associate with SDS and form mixed micelles. Interestingly, the formed mixed micelles apt to attach on the polymer chain and the polymer-bound necklace-like structure forms in the ternary polymer/salt/surfactant system. The structure of the complexes formed in the ternary system is confirmed by 2D NOESY NMR and the interaction mode is proposed. The relations between LCST of different systems and surfactant concentrations are also established quantitatively.

Electronic supplementary material The online version of this article (doi:10.1007/s00396-016-4006-4) contains supplementary material, which is available to authorized users.

✉ Yazhuo Shang
shangyazhuo@ecust.edu.cn

✉ Honglai Liu
hlliu@ecust.edu.cn

[1] State Key Laboratory of Chemical Engineering and Department of Chemistry, East China University of Science and Technology, Shanghai 200237, China

Keywords Surfactants · Thermo-sensitive polymer · Interaction · Salt

Introduction

The interactions between surfactants and water-soluble polymers in aqueous solutions have been extensively studied in the past decades because of their wide applications in various industrial processes and products, such as in pharmaceutical formulations, detergents, oil recovery fluids, cosmetic additives, and food products [1–5]. Mixing surfactants and polymers can generate many interesting functional polymorphic micro- or nano-structures, such as micelles, complexes, vesicles, precipitates, liquid crystals, gels and so on, which have a direct impact on the phase behaviors, rheological, and interfacial properties of mixed systems [6–9]. By far, many fundamental studies have been unfolded for understanding the basic mechanism of the interactions between polymer and surfactant, especially the interaction mode and aggregate behavior that occur at the molecular level in polymer-surfactant mixed systems [10–14]. In exploring polymer-surfactant interactions, two characteristic concentrations have to be mentioned to describe the aggregation process, the critical aggregation concentration (CAC), and the polymer saturation concentration (C_2). The CAC corresponds to the critical surfactant concentration for surfactant-polymer complex formation which is normally smaller than the critical concentration (CMC) of the surfactant in the absence of the polymer, while C_2 indicates the saturation of the polymer chains by micelle-like surfactant aggregates [9, 15]. It has been found that polymer can form mixed aggregates with surfactant, and the aggregate structure depends on the properties of polymer itself, the size of

polar head and hydrophobic tail of the surfactant, the concentrations of components, ionic strength, temperature, etc. [16–19]. However, to our knowledge, the concrete interaction process between polymer and surfactants and the formation mechanism of species in mixed polymer/surfactant systems are controversial, which badly restrict their application in pharmaceutical, cosmetic, and other industrial fields. A detailed understanding of the dependence of the interaction between polymer and surfactant on the properties of surfactant and polymer, the influencing factors, such as the concentrations of components, the added salts, so that to tune the solution properties for specific applications is still a challenge.

In the past decades, numerous kinds of surfactant and polymer have been involved into the mixed polymer/surfactant systems for exploring the interaction between polymer and surfactant. Most of these studies in the literature are focused on the binding interaction between ionic surfactant and oppositely charged polymer due to the strong electrostatic interaction between surfactant and polymer [20–23]. By contrast, little research has been done on the corresponding studies between ionic surfactants and nonionic water-soluble polymers [16, 18, 24–26]. Chauhan and co-workers [18] reported the interactions of the anionic surfactant sodium dodecyl sulfate (SDS) with aqueous polyethylene glycol (PEG), polyvinyl pyrrolidone (PVP), and various PEG + PVP mixtures at different temperatures by applying conductivity, density, and speed of sound techniques. The results showed that the polymers can increase micellar stability drastically and hence decrease CMC values of SDS to a large extent by interacting with SDS, and for all the studied systems, the micellization of SDS is a spontaneous, endothermic, and entropy controlled process. Banipal et al. [16] studied the effect of head groups, temperature, and polymer concentration on surfactant-polyethylene oxide (PEO) interactions using conductivity, surface tension, and viscosity methods. They found that CAC values decrease with polymer concentration and increase with temperature. However, the C_2 values increase with both polymer concentration and temperature for all surfactants, and the presence of the aromatic ring in the head group of surfactant decreases its interaction with PEO, whereas the increased hydrophobicity in surfactant tail strengthens its interaction with PEO. All these studies have shown that the binding interaction between ionic surfactants and nonionic polymers displays much simpler behavior than that between ionic surfactants and oppositely charged polymers due to the absence of strong electrostatic forces and the hydrophobic effects play a significant role as an attractive force producing surfactant micelles that bind to the polymers below their CMC. Meanwhile, the influences of salts on neutral polymer/ionic surfactant systems have attracted increasing attention. The existing studies have shown that the added salt affects the physicochemical properties of the polymer/surfactant mixture in many ways [27–33]. Inorganic salts, such as NaCl, normally decrease the surfactant CAC, and the CAC reduction is enhanced with the increase of salt concentration [29, 30]. This is due to a preferential aggregation of surfactant molecules as a result of screening of the repulsive electrostatic repulsions between surfactant head groups by the excess cations of the added salt. The added inorganic salts also promote the binding affinity and binding ratio of the anionic surfactant to the neutral polymer [31, 32]. This has been explained by a "pseudo-polycation" model, in which a neutral polymer is coordinated with the cations of the added inorganic salt and thus favorably interacts with the anionic surfactant [31, 33]. As for the organic salts, it seems that their effects on the interaction between neutral polymers and ionic surfactants are more complicated. Lin and Hou [13] studied the roles of tetra-n-butylammonium bromide (Bu_4NBr) and tetra-n-propylammonium bromide (Pr_4NBr) in PVP-SDS complexation and proposed the two surfactant aggregation processes. SDS molecules associate with tetraalkylammonium bromides (TAABs) to form mixed micelles, the TAA^+-SDS mixed micelles bind on the PVP chain forming the PVP-(TAA^+-SDS) complex. Their work also reveals that the dominant aggregation in PVP/TAAB/SDS systems is determined by the (SDS)/(TAAB) ratio, and complexation of PVP with SDS does not occur until the(SDS)/(TAAB) ratio is larger than a specific ratio. Obviously, the interaction between polymer and surfactant can be tailed by introducing appropriate organic salts. However, the tuning mechanism is seldom explored.

The thermo-sensitive polymer has caused widespread concern for its sensitivity of the solubility to temperature. The combination of thermo-sensitive polymer and ionic surfactant is bound to have versatile properties and widely application. In this paper, we synthesized the random copolymer poly(2-(2-methoxyethoxy)ethyl methacrylate$_{90}$-co-oligo(ethylene glycol) methacrylate$_{10}$) (P(MEO_2MA_{90}-co-$OEGMA_{10}$)) by atom transfer radical polymerization (ATRP) and characterized the thermally induced aggregation behavior of P(MEO_2MA_{90}-co-$OEGMA_{10}$) in aqueous solution. The interactions between P(MEO_2MA_{90}-co-$OEGMA_{10}$) and an anionic surfactant (SDS) or a cationic surfactant (DTAB) were investigated experimentally. We also examined the effects of the organic salts including Bu_4NBr and Pr_4NBr on the nature of the observed interactions by micropolarity measurements and 2D NOESY NMR experiments. The possible aggregation mechanism of species in P(MEO_2MA_{90}-co-$OEGMA_{10}$)/organic salt/SDS mixed systems were proposed. We hope that our present study may advance our understanding on the general dynamical features and binding mechanism of polymer/ionic surfactant systems.

Materials and methods

Materials

2-(2-methoxyethoxy)ethyl methacrylate (MEO_2MA, purchased from Aldrich with purity 95%) and oligo (ethylene glycol) methacrylate (OEGMA, M_n = 500 g·mol^{-1}, from Aldrich) were purified by passing through a basic aluminum oxide column (200-300 mesh) before use. 1,1,4,7,7-pentamethyldiethylenetriamine (PMDETA, purchased from TCI with purity 98%,), methyl 2-bromopropionate (MBP, purchased from Aldrich with purity 98%), and ethanol (AR, from General-Reagent) were used as received. Copper(I) bromide (Cu^IBr, CP, from Sinopharm Chemical Reagent Co.,Ltd) was washed in acetic acid and ethanol and then dried in a vacuum oven. Sodium dodecyl sulfate (SDS, ACS, from Aladdin), dodecyltrimethylammonium bromide (DTAB, purchased from Aladdin with purity 99%), pyrene (purchased from Aladdin with purity 97%), Ammonium bromide (NH_4Br, purchased from Alfa Aesar with purity above 99%), tetra-n-propylammonium bromide (Pr_4NBr, purchased from Alfa Aesar with purity above 98%), and tetra-n-butylammonium bromide (Bu_4NBr, purchased from Alfa Aesar with purity above 98%) were used as received. D_2O (D-99.9%) was purchased from Aladdin. Ultrapure water (with a resistivity of 18.2 MΩ·cm) was used to prepare all aqueous solutions of surfactants, salts, and polymers.

Synthesis of P(MEO_2MA_{90}-co-$OEGMA_{10}$) random copolymer

The P(MEO_2MA_{90}-co-$OEGMA_{10}$) was synthesized by ATRP according to previous literature reports [34, 35]. MEO_2MA (22.5 mM, 4.15 mL), OEGMA (2.5 mM, 1.16 mL), PMDETA (0.5 mM, 103 μL), and the initiator MBP (0.25 mM, 28 μL) dissolved in ethanol (10 mL) were added in a 25 mL Schlenk flask. After three freeze-pump-thaw cycles, the catalyst Cu^IBr (35.9 mg) was added into the degassed solution. The mixture was heated at 50 °C in an oil bath for 5 h. This reaction was stopped by opening the flask and exposing the catalyst to air. The final mixture was then diluted with ethanol and passed through a neutral alumina column (200-300 mesh) to remove the catalyst Cu^IBr. Then, the filtered solution was diluted with deionized water and subsequently purified by dialysis in water. Finally, after freeze-drying overnight to remove water, the random copolymer was collected (M_n = 2.20 × 10^4 g·mol^{-1}, PDI = 1.63).

Micropolarity measurements

A fluorescence spectrophotometer (Hitachi, F4500) was used to measure the pyrene monomer emission spectrum of pyrene-saturated pure surfactant solution, polymer/surfactant, and polymer/salt/surfactant mixed solutions. The slit widths for excitation and emission were 5 and 2.5 nm, respectively. The excitation wavelength was 335 nm, the scan speed was 240 nm·min^{-1} and the scan range was from 350 to 450 nm. The I_1/I_3 was calculated from the intensity of peak I (at 374 nm) and peak III (at 385 nm) in the pyrene fluorescence spectrum. Pyrene-saturated water was prepared by dissolving 10.0 mg of pyrene in 1000 mL of ultrapure water, and the solution was stirred in the dark at ambient temperature for 24 h. Insoluble pyrene was filtered off, and the pyrene concentration was approximate 7.0 × 10^{-7} M. The pure surfactant solution, polymer/surfactant, and polymer/salt/surfactant mixed solutions were prepared using pyrene-saturated water and kept overnight at room temperature before testing. The SDS concentrations were varied from 0.025 to 100 mM, and the DTAB concentrations were varied from 0.5 to 22 mM.

Dynamic light scattering (DLS)

Particle sizes were measured using a Zetasizer Nano ZS Instrument (Malvern Instruments, UK) equipped with a 4 mW He-Ne laser (λ_0 = 633 nm) and noninvasive back scattering (NIBS) detection at a scattering angle of 173°.The auto correlation function was converted into a volume-weighted particle size distribution using Dispersion Technology Software 5.06 from Malvern Instruments. The samples were stirred to mix thoroughly and kept overnight at room temperature before testing. Each measurement was repeated at least three times. The average result was used as the final hydrodynamic radius (R_h) distribution, and the estimated standard deviation of the R_h values was denoted by error bars.

Turbidity measurements

The aggregation behavior of the polymer in the aqueous solutions was measured in a UV-Vis spectrophotometer (UV-2450, Shimadzu, Japan) between 200 nm and 700 nm using a cuvette with a 2 mm path length. The transmittance of the polymer solutions was monitored in a quartz cuvette (1 cm width) as a function of temperature at a wavelength of 500 nm. Heating and cooling scans were performed between 20 and 70 °C at a scanning rate of 0.1 °C·min^{-1}.

NMR experiments

A Bruker 400 MHz NMR spectrometer instrument was used for all NMR experiments at 298.0 K. All NMR data were processed using the software package MestReNov. 6.1.0. The proton and 2D NOESY NMR spectra of the polymer, salts, and surfactant were measured using D_2O or $CDCl_3$ as the solvent, and all samples were stirred to mix thoroughly and kept overnight at room temperature before the measurement.

Results and discussion

Thermo-responsive behaviors of P(MEO_2MA_{90}-co-$OEGMA_{10}$) random copolymer in aqueous solution

Using MBP as initiator and Cu^IBr/PMDETA as catalyst, P(MEO_2MA_{90}-co-$OEGMA_{10}$) random copolymer is synthesized by ATRP of MEO_2MA and OEGMA in ethanol at 50 °C. ^1H NMR result (Fig. 1a) confirms the structure of P(MEO_2MA_{90}-co-$OEGMA_{10}$). $PMEO_2MA$ and POEGMA are both thermo-responsive homopolymers that dissolve molecularly at 24 and 90 °C in aqueous solution, respectively, but precipitate above their LCSTs. As expected, the P(MEO_2MA_{90}-co-$OEGMA_{10}$) has the similar solubility and thermo-responsive behavior in aqueous solution, and its LCST is between that of $PMEO_2MA$ and POEGMA. Figure 1b shows the temperature-dependent transmittance and hydrodynamic radii of P(MEO_2MA_{90}-co-$OEGMA_{10}$). The random copolymer is molecularly soluble in water at temperatures below 38 °C, as indicated by the nearly constant transmittance at about 100%. Meanwhile, the R_h values of P(MEO_2MA_{90}-co-$OEGMA_{10}$) are around 7 nm under 38 °C suggesting polymer chains are molecularly dissolved, which is consistent with the transmittance results. When temperature is above 38 °C, the transmittance decreases to 0% dramatically, and the hydrodynamic radii are constantly maintained at about 1000 nm. The turbidity measurement results are coincidence with the dynamic light scattering analysis indicating the formation of the large aggregations. Obviously, the LCST of the prepared P(MEO_2MA_{90}-co-$OEGMA_{10}$) is 38 °C. Furthermore, the negligible hysteresis obtained from the heating and cooling cycles of the temperature-dependent transmittance suggests that the studied thermo-responsive polymer has a good reversibility. The appreciably reversible thermal responsivity of P(MEO_2MA_{90}-co-$OEGMA_{10}$) should be attributed to a delicate balance between hydrogen bonds between the copolymers and water molecules and hydrophobic interactions of polymer segments. If the balance is broken, the polymers attain a new thermodynamic equilibrium by spontaneously changing the extent of aggregation [34].

Interaction between P(MEO_2MA_{90}-co-$OEGMA_{10}$) and surfactants in aqueous solutions

SDS and DTAB are widely used in many kinds of industries because of their good emulsification property, foamability, lubrication, and dispersibility. Therefore, the SDS and DTAB are selected as objects to explore the interaction between P(MEO_2MA_{90}-co-$OEGMA_{10}$) and surfactants in the present study.

P(MEO_2MA_{90}-co-$OEGMA_{10}$)-SDS interactions

Micropolarity measurement using pyrene as a probe is a simple and easy way to understand the aggregation process of polymer and surfactant when exploring the interactions between polymer and surfactant. The intensity ratio of the emission of pyrene at 374 and 385 nm (I_1/I_3) is quite sensitive to the polarity of pyrene surroundings. The plot of I_1/I_3 against surfactant concentrations can be used to monitor the formation of surfactant micelles and polymer-bound surfactant aggregates in aqueous solutions [14, 36, 37]. Figure 2a presents the plots of I_1/I_3 ratio against surfactant concentration (C_{SDS}) for SDS and P(MEO_2MA_{90}-co-$OEGMA_{10}$)/SDS aqueous solutions. The concentration of P(MEO_2MA_{90}-co-$OEGMA_{10}$) keeps constant (1 $g{\cdot}L^{-1}$). For pure SDS aqueous solution, the I_1/I_3 has no obvious changes when SDS concentration is

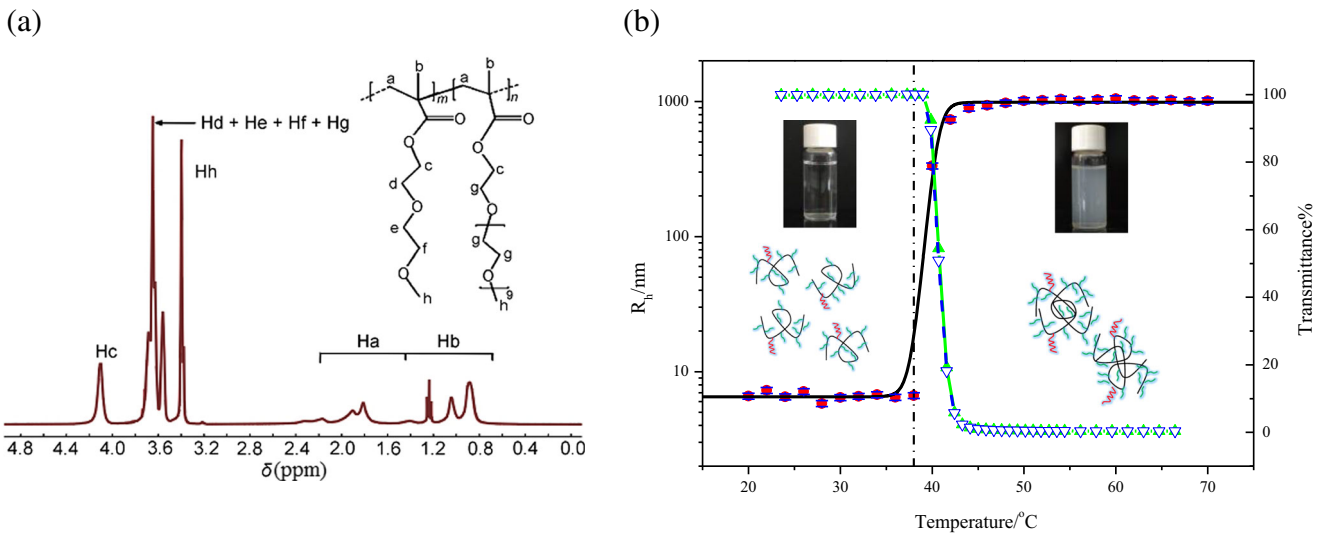

Fig. 1 **a** ^1H NMR spectra of P(MEO_2MA_{90}-co-$OEGMA_{10}$) in $CDCl_3$. **b** DLS and turbidity measurements in aqueous solutions of P(MEO_2MA_{90}-co-$OEGMA_{10}$) random copolymer. The *dots* represent the hydrodynamic radii. The *solid* and *open triangles* represent the heating and cooling cycles of temperature-dependent transmittance

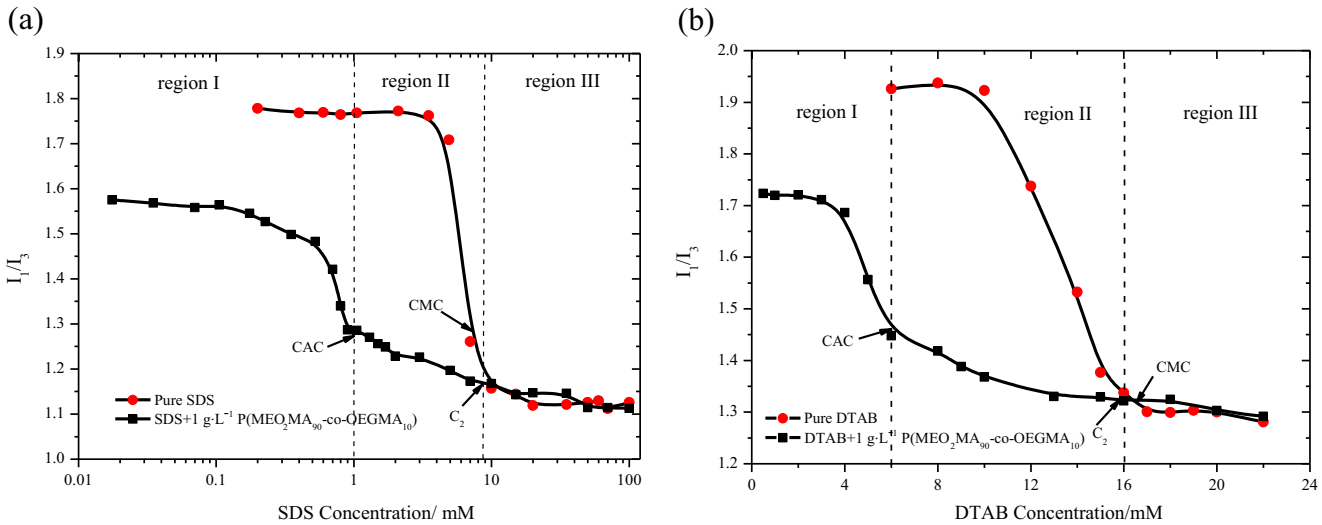

Fig. 2 Plots of pyrene I_1/I_3 ratio against surfactant concentrations for pure surfactant and P(MEO_2MA_{90}-co-$OEGMA_{10}$)/surfactant solutions. **a** SDS. **b** DTAB. The I_1/I_3-$C_{surfactant}$ curve (*squared black line*) of the P(MEO_2MA_{90}-co-$OEGMA_{10}$)/surfactant system can be divided into three stages (I, II, and III) by two characteristic surfactant concentrations, CAC and C_2

relatively low (lower than 7 mM). However, when SDS concentration reaches about 7 mM, the I_1/I_3 decreases dramatically. This means SDS micelles have formed, and this concentration represents the CMC of SDS.

Compared with the pure SDS system, the situation of P(MEO_2MA_{90}-co-$OEGMA_{10}$)/SDS system is more complicated. It can be seen that the variation of I_1/I_3 with C_{SDS} appears three different stages (I, II, and III) according to the dividing point of two characteristic concentrations, CAC and C_2. These three stages represent three different modes of the interaction between P(MEO_2MA_{90}-co-$OEGMA_{10}$) and SDS. [37] At lower surfactant concentration (C_{SDS} < 1 mM), the I_1/I_3 keeps constant first and then decreases dramatically when SDS concentration reaches the CAC (ca. 1 mM), at which the SDS molecules begin to bind on the P(MEO_2MA_{90}-co-$OEGMA_{10}$) chain to form micelle-like SDS aggregates. Further increase SDS concentration (1 mM < C_{SDS} < 9 mM), the second stage occurs; more and more polymer-bound SDS aggregates are formed until the polymer is saturated when SDS concentration is about 9 mM (C_2). The I_1/I_3 value in this stage varies slightly from 1.28 to 1.17, indicating that the changes of inside polarity for the studied system are almost negligible. Therefore, polarity index (I_1/I_3) of 1.28-1.17 can be considered as the characteristic I_1/I_3 value for the P(MEO_2MA_{90}-co-$OEGMA_{10}$)-bound SDS complexes in the absence of added salts. In stage III (C_{SDS} > 9 mM), the I_1/I_3 decreases slowly from 1.17 to ca. 1.10, showing that free SDS micelles are formed and coexist with the P(MEO_2MA_{90}-co-$OEGMA_{10}$)-bound SDS complexes [14]. Based on the above analysis, the aggregation process of P(MEO_2MA_{90}-co-$OEGMA_{10}$) and SDS depended on the SDS concentrations is illustrated in Fig. 3. Similar results are also observed in mixed systems of SDS/PEO and SDS/PVP [38, 39]. The hydrophobic interaction is the main driving force of the binding between nonionic polymer and ionic surfactant.

The above analysis has proved that the surfactant SDS can interact with P(MEO_2MA-co-OEGMA) by different modes depending on surfactant concentration. Our previous study

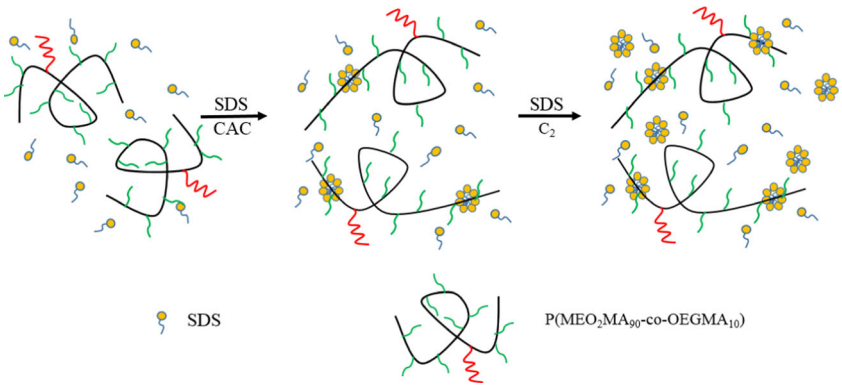

Fig. 3 Schematic illustration of the aggregation process in P(MEO_2MA_{90}-co-$OEGMA_{10}$)/SDS system

has also shown that the P(MEO_2MA-co-OEGMA) has the thermo-induced aggregation behavior and its LCST correlates linearly with the mole fraction of OEGMA units in the copolymer [34]. The introduction of SDS to polymer system must affect the thermo-sensitive behavior of polymer itself and further affect the application of polymer. Based on above, the influence rule of SDS on thermo-sensitive behavior of polymer and the corresponding mechanism are revealed in the present study.

Figure 4a provides the variation of R_h of species existed in the mixed solutions of P(MEO_2MA_{90}-co-$OEGMA_{10}$)/SDS (concentration of polymer is 1g·L^{-1} and the SDS concentration is variable) as a function of temperature. The temperature at which the R_h of species changes dramatically is specified as the LCST of polymer and the large aggregates are formed when the temperature above the LCST. The detailed results are listed in Table 1. It can be seen that the LCST of P(MEO_2MA_{90}-co-$OEGMA_{10}$) is 38 °C when SDS is absent. However, with the addition of surfactant SDS, the LCST of the P(MEO_2MA_{90}-co-$OEGMA_{10}$)/SDS mixed system increase gradually. At the same time, the R_h of species in system becomes smaller and smaller after the phase transition, and the

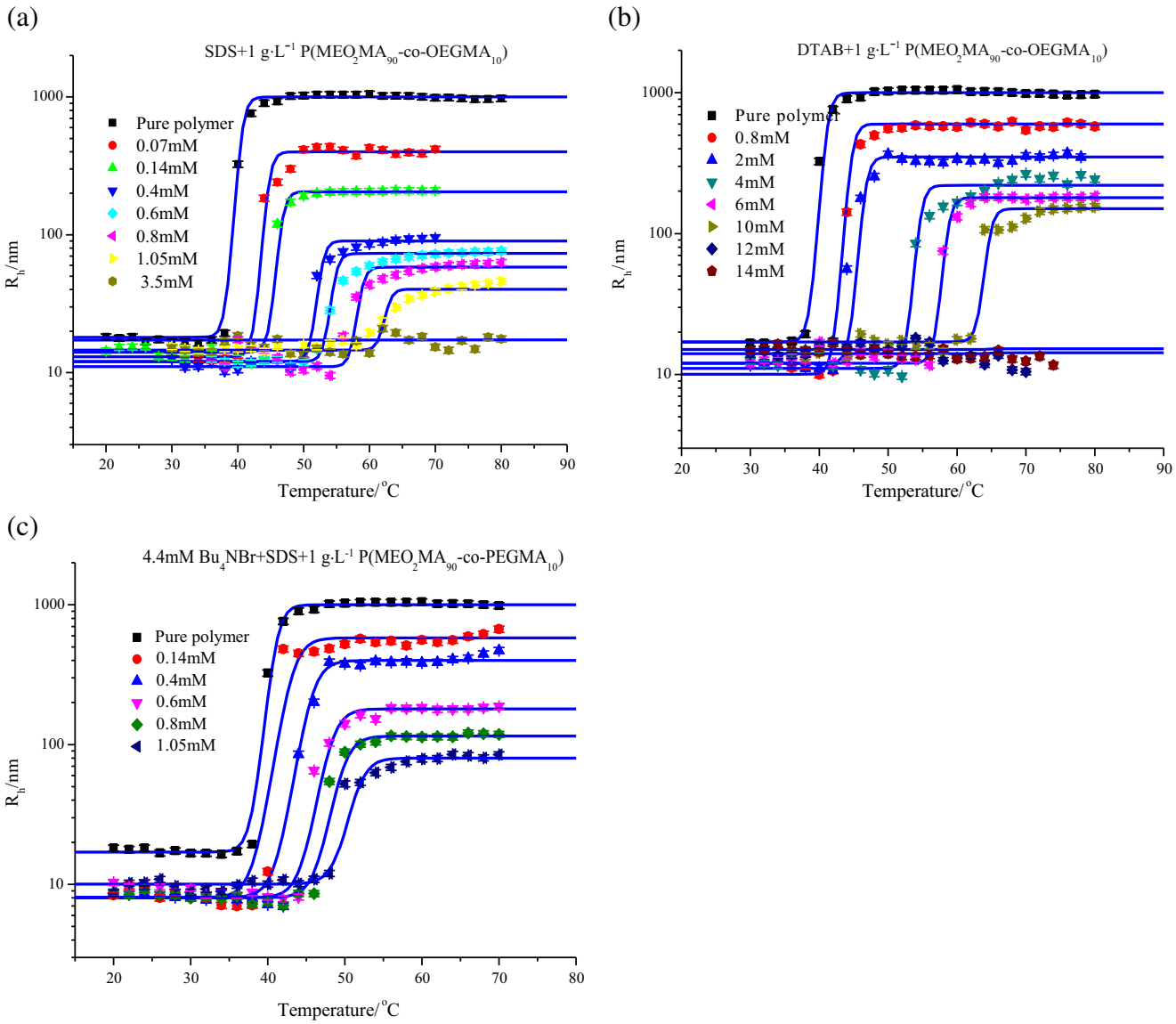

Fig. 4 Plots of R_h as a function of temperature in **a** P(MEO_2MA_{90}-co-$OEGMA_{10}$)/SDS, **b** P(MEO_2MA_{90}-co-$OEGMA_{10}$)/DTAB, and **c** P(MEO_2MA_{90}-co–$OEGMA_{10}$)/Bu_4NBr/SDS systems. The concentration of P(MEO_2MA_{90}-co-$OEGMA_{10}$) is 1 g·L^{-1}. The SDS concentrations are varied from **a** 0.07 to 3.5 mM and **c** 0.14 to 1.05 mM, respectively, and the DTAB concentrations are varied from 0.8 to 14 mM

Table 1 Phase transition of the P(MEO_2MA_{90}-co-$OEGMA_{10}$) with different concentrations of SDS with and without Bu_4NBr in the aqueous solutions

C_{SDS}/mM	LCST/°C		R_h[a]/nm	
	without salt	4.4 mM Bu_4NBr	without salt	4.4 mM Bu_4NBr
0	38	38	1000	1000
0.07	42	not tested	400	not tested
0.14	44	40	205	550
0.4	50	42	90	400
0.6	52	44	73	180
0.8	56	46	58	115
1.05	60	48	40	80
3.5	–	not tested	17	not tested

[a] R_h of P(MEO_2MA_{90}-co-$OEGMA_{10}$) is measured by DLS above LCST. $C_{P(MEO2MA90\text{-}co\text{-}OEGMA10)}$ = 1 g·L^{-1}. The concentration of Bu_4NBr is 4.4 mM

difference between the particle sizes before and after the LCST is getting less stark. Obviously, when the SDS concentration is higher than 1 mM, the particle sizes are almost equal within the studied temperature range, namely the phase transition disappear and the polymer loses its thermo-sensitive properties in the mixed system with higher SDS concentration. Our previous study has shown that the thermal responsivity of P(MEO_2MA_{90}-co-$OEGMA_{10}$) is derived from the existence of both hydrogen bonds between the copolymers and water molecules and hydrophobic interactions of polymer segments [34]. For the P(MEO_2MA_{90}-co-$OEGMA_{10}$)/SDS mixed system, however, the addition of SDS enhances the complexity of interactions among compositions in systems. First of all, the electrostatic repulsion among the SDS head groups cannot be neglected. The existence of electrostatic repulsion among the surfactants attached on the polymer chains hindered the aggregation of hydrophobic interactions of polymer segments. Secondly, the hydrophilic head groups of the surfactants attached on polymers have the potential of "locking water" and thus inhibit the loss of water connecting with polymers by hydrogen bonding. Obviously, the process of phase transition, namely the break of hydrogen bonding between polymers and water molecules to the aggregation of polymer due to the hydrophobic interactions of polymer segments, is retarded, and thus LCST increases. Electrostatic repulsion effect and the "locking water" effect caused by surfactant head groups affect the thermal responsivity of polymer simultaneously. When the SDS concentration is over CAC (ca. 1 mM), the electrostatic repulsion among the premicelles attached on the polymer chain and their "locking water" effect are strong enough to hinder the aggregation of polymer hydrophobic chains effectively. Correspondingly, the temperature-responsive aggregation phenomenon becomes less obvious. Further increase SDS concentration, the aggregation of polymer hydrophobic segments is inhibited completely, and the thermally induced phase transition behavior disappears.

P(MEO_2MA_{90}-co-$OEGMA_{10}$)-DTAB interactions

The above analysis has shown that the properties of charged hydrophilic head group of surfactant determine the thermal responsivity of polymer to a large extent. Here, the cationic surfactant DTAB with the same alkyl chain length as anionic surfactant SDS was selected to study the interaction between polymer and surfactant. Figure 2b provides the variation of I_1/I_3 with DTAB concentration for DTAB and P(MEO_2MA_{90}-co-$OEGMA_{10}$)/DTAB aqueous solutions. As seen in Fig. 2b, just as the situation of system containing SDS, the two characteristic concentrations, CAC (6 mM) and C_2 (16 mM) are determined using micropolarity experiments. These values are much higher than those of corresponding SDS system, suggesting that DTAB has poorer capacity of self-aggregation and weaker interaction with P(MEO_2MA_{90}-co-$OEGMA_{10}$) than SDS.

Table 2 Phase transition of the P(MEO_2MA_{90}-co-$OEGMA_{10}$) with different concentrations of DTAB in the aqueous solutions

C_{DTAB}/mM	LCST/°C	R_h[a]/nm
0	38	1000
0.8	42	600
2	46	350
4	52	220
6	56	180
10	62	150
12	–	15
14	–	14

[a] R_h of P(MEO_2MA_{90}-co-$OEGMA_{10}$) is measured by DLS above LCST. $C_{P(MEO2MA90\text{-}co\text{-}OEGMA10)}$ = g·L^{-1}

Similarly, the effect of DTAB concentration on the LCST of P(MEO_2MA_{90}-co-$OEGMA_{10}$)/DTAB system is studied using DLS (Fig. 4b), and the detailed results are listed in Table 2. Compared with P(MEO_2MA_{90}-co-$OEGMA_{10}$)/SDS system, the phase transition temperature of P(MEO_2MA_{90}-co-$OEGMA_{10}$)/DTAB system increases slightly with addition of DTAB, and the hydrodynamic radius of aggregates formed above LCST is larger. It seems that the ability of DTAB to prevent the aggregation of polymer chains and "locking water" effect is weaker than that of SDS, which should be attributed to the poorer capacity of self-aggregation and weaker interaction with P(MEO_2MA_{90}-co-$OEGMA_{10}$) of DTAB.

Interactions between P(MEO_2MA_{90}-co-$OEGMA_{10}$) and SDS in brine

In biological and pharmaceutical processes, polymer/surfactant mixtures are always used in salt environments. So, it is necessary to understand the roles of salt in the polymer/salt/surfactant system. In this work, the inorganic salt NH_4Br, organic salts Pr_4NBr, and Bu_4NBr are specified to study the effect of salt on the interaction of polymer and surfactant.

Figure 5 shows the I_1/I_3-C_{SDS} curves of P(MEO_2MA_{90}-co-$OEGMA_{10}$)/salt/SDS systems with different salts. However, no matter what kind of salt is introduced into the P(MEO_2MA_{90}-co-$OEGMA_{10}$)/SDS system, the I_1/I_3-C_{SDS} curves of all systems converge at the concentration of SDS about 1 mM which correspond to the CAC of SDS. Due to the same polarity of these systems at this point, the structure of complexes attached on the polymer chains in the P(MEO_2MA_{90}-co-$OEGMA_{10}$)/salt/SDS systems is similar to that of P(MEO_2MA_{90}-co-$OEGMA_{10}$)/SDS system. This deduction is confirmed by the NMR experiments in the following sections.

It can be seen from Fig. 5, the addition of inorganic salt (NH_4Br) has no obvious effect on the curves of I_1/I_3-C_{SDS}, and however, the effect of organic salts is significant. Obviously, the addition of organic salts changes the typical interaction between P(MEO_2MA_{90}-co-$OEGMA_{10}$) and SDS. In order to explore the influencing mechanism of organic salts on the interaction between P(MEO_2MA_{90}-co-$OEGMA_{10}$) and SDS, the P(MEO_2MA_{90}-co-$OEGMA_{10}$)/Bu_4NBr/SDS system (C_{Bu4NBr} = 4.4 mM) was singled out for further study.

The thermo-induced phase transition behavior of P(MEO_2MA_{90}-co-$OEGMA_{10}$) in P(MEO_2MA_{90}-co-$OEGMA_{10}$)/Bu_4NBr/SDS mixed system (C_{Bu4NBr} = 4.4 mM) was studied using DLS. Figure 4c shows the variation of R_h of species in P(MEO_2MA_{90}-co-$OEGMA_{10}$)/Bu_4NBr/SDS solutions with temperature. Similarly, the concentration of P(MEO_2MA_{90}-co-$OEGMA_{10}$) keeps constant (1 g·L^{-1}). The detailed results are listed in Table 1.

Figure 4c reveals that the P(MEO_2MA_{90}-co-$OEGMA_{10}$) has the same thermally induced aggregation behavior in P(MEO_2MA_{90}-co-$OEGMA_{10}$)/Bu_4NBr/SDS solution as in P(MEO_2MA_{90}-co-$OEGMA_{10}$)/SDS aqueous solution. However, the addition of Bu_4NBr changed the LCST of P(MEO_2MA_{90}-co-$OEGMA_{10}$) significantly. The LCST of P(MEO_2MA_{90}-co-$OEGMA_{10}$) in system with Bu_4NBr is much lower than that in system without Bu_4NBr. Meanwhile, the hydrodynamic radius of species formed

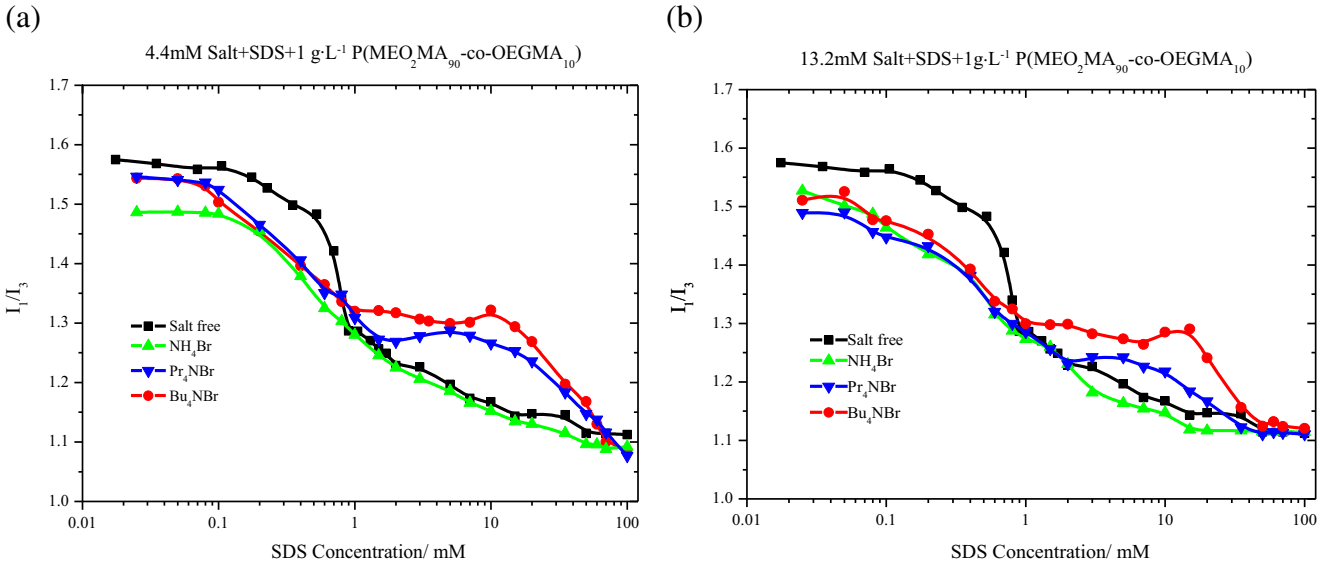

Fig. 5 Plots of pyrene I_1/I_3 ratio against C_{SDS} for P(MEO_2MA_{90}-co-$OEGMA_{10}$)/salt/SDS solutions. The salts include NH_4Br, Pr_4NBr, and Bu_4NBr. The concentrations of salt are **a** 4.4 mM and **b** 13.2 mM. The concentration of P(MEO_2MA_{90}-co-$OEGMA_{10}$) is 1 g·L^{-1}

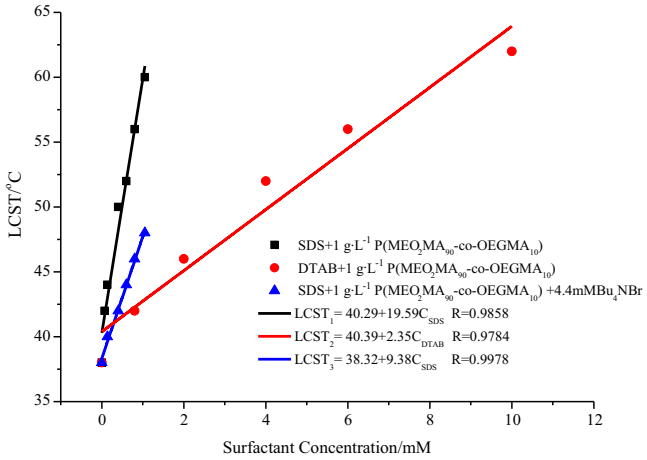

Fig. 6 Standard curve of the measured LCST as a function of surfactant concentration (C_{SDS} or C_{DTAB}) for P(MEO_2MA_{90}-co-$OEGMA_{10}$) in aqueous solutions with and without salt. 0 mM < C_{SDS} < 1.05 mM; 0 mM < C_{DTAB} < 10 mM

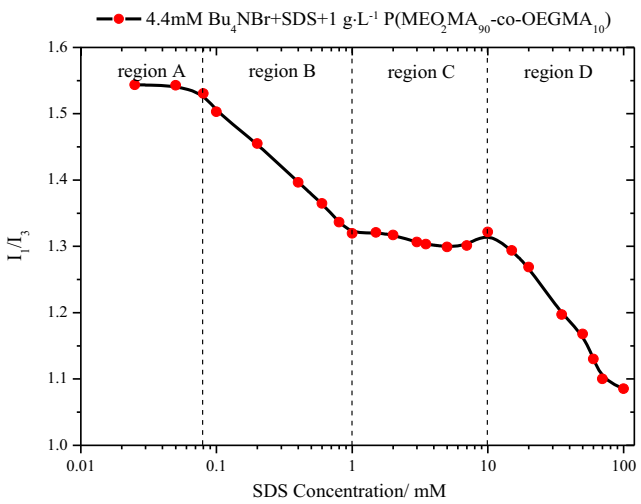

Fig. 7 Plot of the pyrene I_1/I_3 ratio of P(MEO_2MA_{90}-co-$OEGMA_{10}$)/Bu_4NBr/SDS system (C_{Bu4NBr} = 4.4 mM) as a function of the SDS concentrations

in system with Bu_4NBr is much larger than that of in system without Bu_4NBr when the temperature is above the corresponding LCST. The addition of Bu_4NBr can hinder the combination of P(MEO_2MA_{90}-co-$OEGMA_{10}$) and SDS by the electrostatic interaction and thus result in the smaller resistance among the polymer chains in the aggregation process. As a result, compared to that in aqueous solution, the association of P(MEO_2MA_{90}-co-$OEGMA_{10}$) increases; lower LCST and larger aggregates are observed.

Based on the above experiments, the relations between LCST of different systems and surfactant concentrations were established, as shown in Fig. 6. The simple linear relations between LCST and surfactant concentration for all systems were found and can be precisely described by the following equations:

$$\mathrm{LCST}_1 = 40.29 + 19.59\mathrm{C}_{SDS}(0mM < \mathrm{C}_{SDS} < 1.05mM, \mathrm{P(MEO_2MA_{90}-co-OEGMA_{10})/SDS}) \quad (1)$$

$$\mathrm{LCST}_2 = 40.39 + 2.35\mathrm{C}_{\mathrm{DTAB}}(0mM < \mathrm{C}_{\mathrm{DTAB}} < 10mM, \mathrm{P(MEO_2MA_{90}-co-OEGMA_{10})/DTAB}) \quad (2)$$

$$\mathrm{LCST}_3 = 38.32 + 9.38\mathrm{C}_{SDS}(0mM < \mathrm{C}_{SDS} < 1.05mM, \mathrm{P(MEO_2MA_{90}-co-OEGMA_{10})/Bu_4NBr/SDS}) \quad (3)$$

Obviously, the slopes of these lines reveal the strength of the interaction between P(MEO_2MA_{90}-co-$OEGMA_{10}$) and surfactant in aqueous solutions with and without salt. According to these equations, it can be seen that the LCST of the system containing P(MEO_2MA_{90}-co-$OEGMA_{10}$) could be tuned to the expected temperatures by simply introducing slightly surfactants, salts, or both of them to the system.

Figure 7 illustrates the changes of I_1/I_3 with SDS concentration of P(MEO_2MA_{90}-co-$OEGMA_{10}$)/Bu_4NBr/SDS system. Compared with the situation of system without Bu_4NBr (Fig. 2a), we can see that the I_1/I_3-C_{SDS} curve for P(MEO_2MA_{90}-co-$OEGMA_{10}$)/Bu_4NBr/SDS (C_{Bu4NBr} = 4.4 mM) system has been divided into four distinct stages (stages A, B, C, and D). With the increase of SDS concentration, the I_1/I_3 undergoes constant, decrease, constant, and decrease again, respectively. In the first stage, namely stage A (C_{SDS} < 0.08 mM), I_1/I_3 is maintaining a constant value of about 1.55, indicating that no distinct hydrophobic microdomains are formed in the solution. Almost all species in solutions, including SDS, Bu_4NBr, and P(MEO_2MA_{90}-co-$OEGMA_{10}$) exist in the state of monomer, and no interaction among polymer, SDS, and Bu_4NBr is explored. With the increase of surfactant concentration (0.08 mM < C_{SDS} < 1.0 mM), as can be seen in stage B, I_1/I_3 deceases dramatically. It is worth mentioning that the concentration at which the I_1/I_3 start decrease significantly (C_{SDS} = 0.08 mM) corresponds to the CMC of the Bu_4N^+-SDS mixed solution [36]. This implies that the Bu_4N^+-SDS mixed micelles should be formed under this condition due to the electrostatic interaction and hydrophobic interaction between SDS and Bu_4NBr. Furthermore, it is observed that the I_1/I_3 values are located in the range of 1.55 to 1.32, which is apparently different from the characteristic

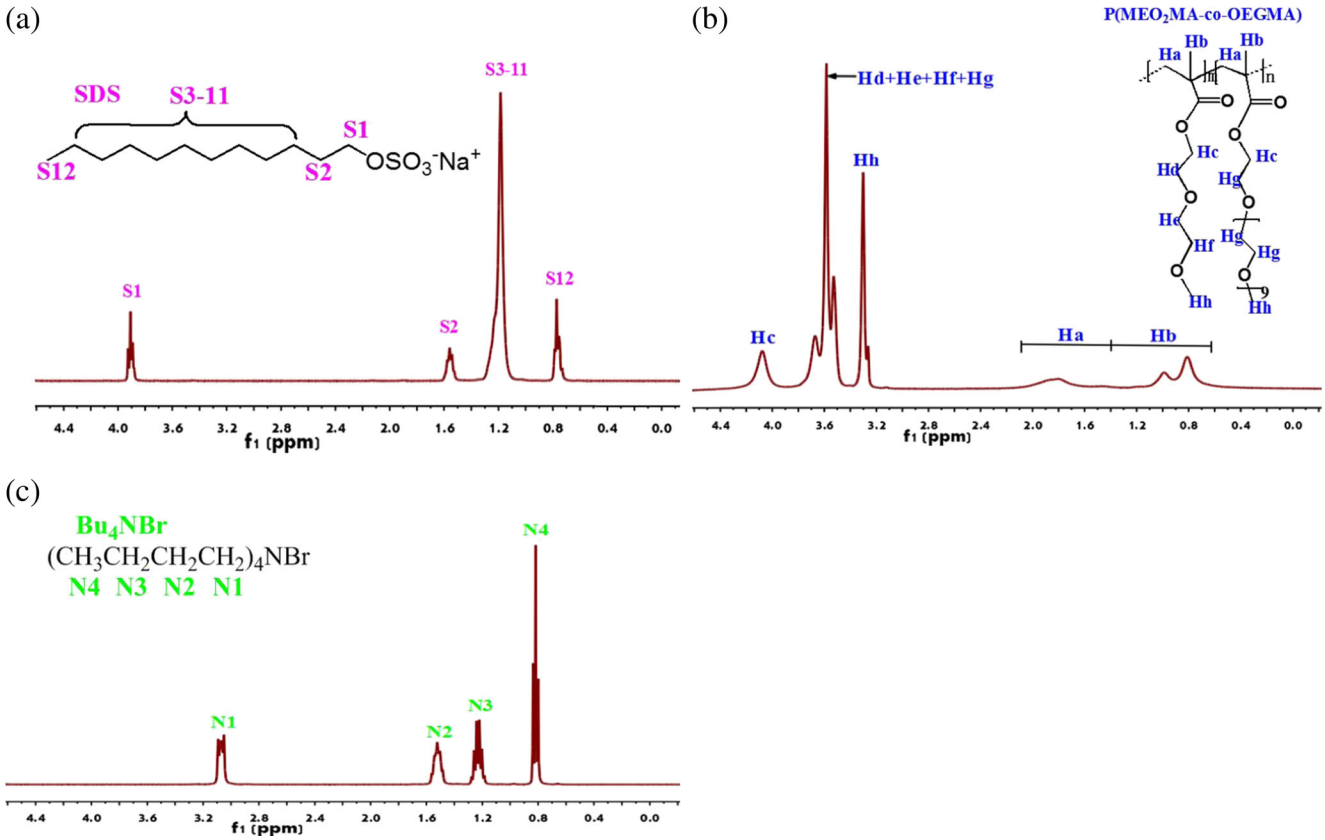

Fig. 8 ^{1}H NMR spectra of **a** SDS, **b** P(MEO_2MA_{90}-co-$OEGMA_{10}$), and **c** Bu_4NBr in D_2O

polarity index value for the P(MEO_2MA_{90}-co-$OEGMA_{10}$)-bound SDS complexes (the I_1/I_3 values are within the range of 1.28 to 1.17). It looks like that the interaction is not obvious in this stage.

Further increase of the SDS concentration (1.0 mM < C_{SDS} < 10 mM), as shown in stage C, the values of I_1/I_3 keep almost constant. In principle, if there are two or more different hydrophobic microdomains with different polarities in the aqueous phase, pyrene molecules will be partitioned into these microenvironments [40, 41]. So the observed I_1/I_3 values should be considered as a weighted average of the polarity in these different hydrophobic microdomains. The slight change of I_1/I_3 from 1.32 to 1.30 indicates that the microdomains of new species should have the similar polarity to that of the Bu_4N^+-SDS mixed micelles once they are formed in solutions. We speculate maybe the Bu_4N^+-SDS mixed micelles are bonding to the polymers gradually during the course of increasing SDS concentration. The existence of new species of P(MEO_2MA_{90}-co-$OEGMA_{10}$)-bound Bu_4N^+-SDS complexes has been confirmed by the NMR experiments in the following sections. It can be concluded that Bu_4N^+-SDS mixed micelles coexist with P(MEO_2MA_{90}-co-$OEGMA_{10}$)-bound Bu_4N^+-SDS complexes in the solutions in stage C.

In Fig. 5a, b, the level in the I_1/I_3 begins and ends at the same SDS concentration (ca. 1.0 and 10 mM), regardless of the concentration of Bu_4NBr. Consequently, in the presence of Bu_4NBr, the adsorption of SDS molecules onto P(MEO_2MA_{90}-co-$OEGMA_{10}$) is directly related to the SDS concentration. When the SDS concentration is higher than 10 mM, as can be seen in stage D (10 mM < C_{SDS} < 100 mM), the I_1/I_3 decreases dramatically until to about 1.1 that coincide with the characteristic polarity index of 1.28-1.17 for the P(MEO_2MA_{90}-co-$OEGMA_{10}$)-bound SDS complexes when the SDS concentration is over 50 mM. This reveals that the average polarity of the hydrophobic microdomains in region D for the studied system is similar to that of the hydrophobic microdomains produced by free SDS micelles and P(MEO_2MA_{90}-co-$OEGMA_{10}$)-bound SDS complexes. Obviously, the higher of the SDS concentration (higher than 50 mM), the less obvious of the Bu_4NBr effect on the P(MEO_2MA_{90}-co-$OEGMA_{10}$)/SDS system. Correspondingly, the interaction behavior of the P(MEO_2MA_{90}-co-$OEGMA_{10}$)/Bu_4NBr/SDS system is almost equivalent to that of P(MEO_2MA_{90}-co-$OEGMA_{10}$)/SDS system when SDS concentration is higher.

The above analysis has shown that the species formed in the P(MEO_2MA_{90}-co-$OEGMA_{10}$)/Bu_4NBr/SDS system are variable with SDS concentration. The 2D NOESY experiments are used to further identify the formation and microstructure of these species. The 2D NOESY NMR is a useful technique for elucidating the microstructure of a polymer-surfactant complex, and it has been applied to investigate polymer penetration into surfactant

aggregates in aqueous media [10–12, 14, 42]. The ^{1}H NMR spectra of SDS, P(MEO_2MA_{90}-co-$OEGMA_{10}$), and Bu_4NBr in D_2O are shown in Fig. 8. Referring to the results obtained by micropolarity measurements (Fig. 7), three samples which characterize different stages of P(MEO_2MA_{90}-co-$OEGMA_{10}$)/Bu_4NBr/SDS system (SDS concentrations are 0.8, 8, 20 mM, respectively) are selected for the 2D NOESY analysis; the results have been shown in Fig. 9.

Figure 9a provides the information on the microstructure of species formed in P(MEO_2MA_{90}-co-$OEGMA_{10}$)/Bu_4NBr/SDS system when SDS concentration is 0.8 mM. The clear cross-peaks between Bu_4N^+ N1 and N2 protons and SDS S3–11 protons indicate the formation of the Bu_4N^+-SDS mixed micelles, and the Bu_4N^+ ions are not only attached to the micellar surface but also inserted into the micellar interior of mixed micelles in region B.

In Fig. 9b (C_{SDS} = 8 mM, region C), the patterns of intramolecular and intermolecular cross-peaks arising from Bu_4N^+ ion and SDS are identical to those shown in Fig. 9a, indicating the Bu_4N^+-SDS mixed micelles still exist in region C. In addition, the weak NOE cross-peaks between the P(MEO_2MA_{90}-co-$OEGMA_{10}$) protons and the SDS protons (S3–11) shown in Fig. 9b indicate that the P(MEO_2MA_{90}-co-$OEGMA_{10}$) only has weak interaction with SDS. Thus, for the P(MEO_2MA_{90}-co-$OEGMA_{10}$)/Bu_4NBr/SDS system, the lack of direct NOE cross-peaks between P(MEO_2MA_{90}-co-$OEGMA_{10}$) and SDS suggests that the P(MEO_2MA_{90}-co-$OEGMA_{10}$) chain does not penetrate into the region occupied by the SDS alkyl chains and only tangle through the surface of P(MEO_2MA_{90}-co-$OEGMA_{10}$)-bound SDS complexes. This is similar to that complexes formed in the P(MEO_2MA_{90}-co-$OEGMA_{10}$)/SDS system. So, there is a coincident point in Fig. 5. In the presence of Bu_4NBr, due to the NOESY data,

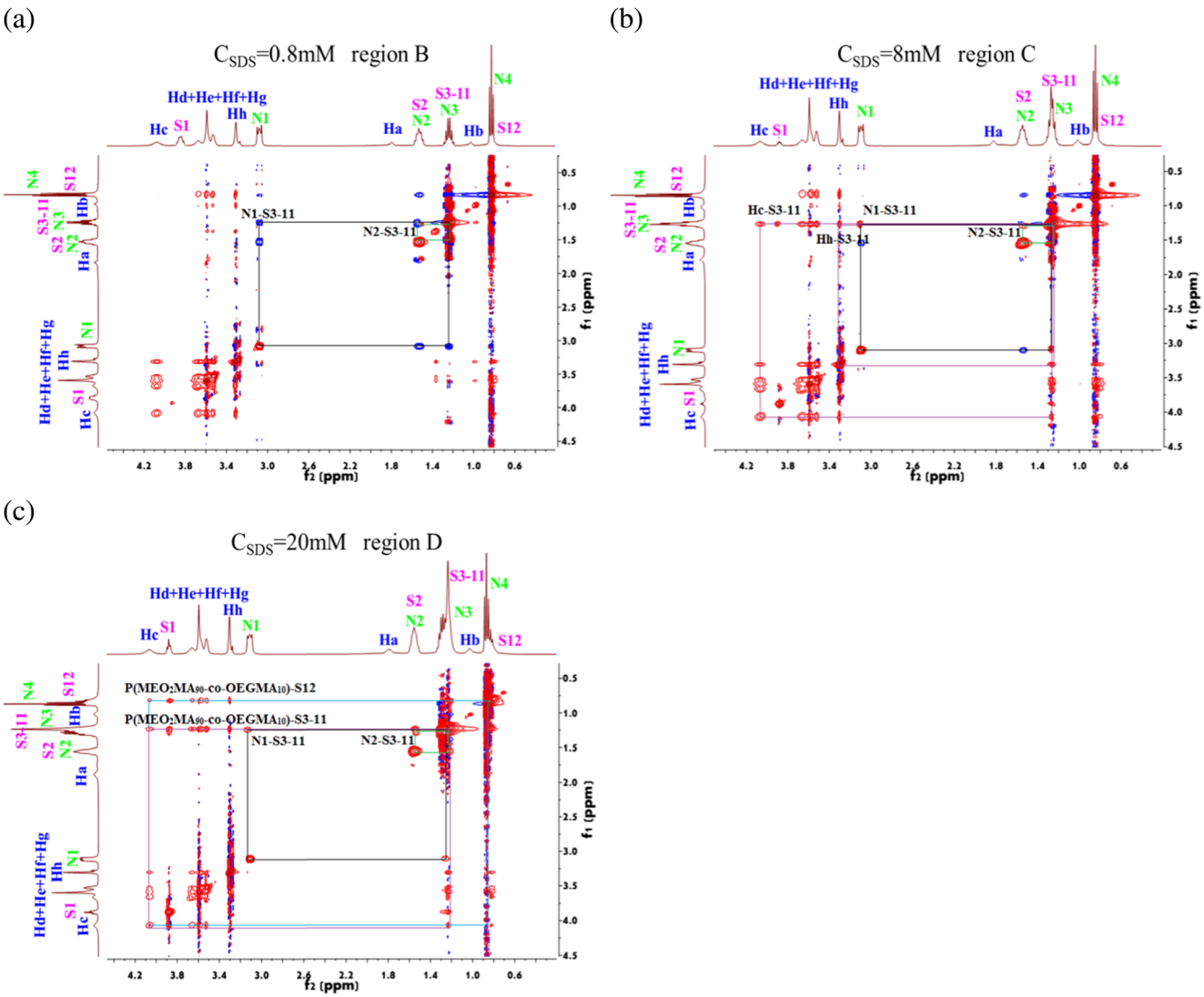

Fig. 9 2D NOESY spectra of P(MEO_2MA_{90}-co-$OEGMA_{10}$)/Bu_4NBr/SDS solutions in D_2O.C_{SDS} = **a** 0.8 mM (region B). **b** 8 mM (region C). **c** 20 mM (region D). The concentrations of P(MEO_2MA_{90}-co-$OEGMA_{10}$) and Bu_4NBr are 1 g·L^{-1} and 4.4 mM, respectively

it can be concluded that, free Bu_4N^+-SDS mixed micelles and P(MEO_2MA_{90}-co-$OEGMA_{10}$)-bound Bu_4N^+-SDS complexes coexist in the solution of P(MEO_2MA_{90}-co-$OEGMA_{10}$)/Bu_4NBr/SDS when SDS concentration is located in region C. It should be noted that no cross-peaks between P(MEO_2MA_{90}-co-$OEGMA_{10}$) and Bu_4NBr can be observed, suggesting that the P(MEO_2MA_{90}-co-$OEGMA_{10}$) chain is not in proximity to the Bu_4N^+ ions even though the Bu_4N^+ ions are absorbed on the P(MEO_2MA_{90}-co-$OEGMA_{10}$)-bound Bu_4N^+-SDS complexes.

The 2D NOESY spectrum in Fig. 9c shows that all SDS protons have cross-peaks with P(MEO_2MA_{90}-co-$OEGMA_{10}$) protons when SDS concentration is 20 mM in the P(MEO_2MA_{90}-co-$OEGMA_{10}$)/Bu_4NBr/SDS system. Specifically, the presence of cross-peaks between P(MEO_2MA_{90}-co-$OEGMA_{10}$) and S12 suggests that the P(MEO_2MA_{90}-co-$OEGMA_{10}$) chain penetrates into the core of the polymer-bound Bu_4N^+-SDS complexes. The positive NOE correlation among the protons of the Bu_4N^+ ion and clear cross-peaks between Bu_4N^+ N1 and N2 protons and SDS S3–11 protons in Fig. 9c indicates that there must be free Bu_4N^+-SDS mixed micelles exist in region D. Obviously, the P(MEO_2MA_{90}-co-$OEGMA_{10}$) chain penetrates into the core of the polymer-bound Bu_4N^+-SDS complexes and also coexists with free Bu_4N^+-SDS mixed micelles in stage D. Similar results are also found in the P(MEO_2MA_{90}-co-$OEGMA_{10}$)/Pr_4NBr/SDS system (Figure S1 and S2). According to the analysis of the micropolarity and 2D NOESY NMR measurements, the schematic illustration of the aggregation process in P(MEO_2MA_{90}-co-$OEGMA_{10}$)/Bu_4NBr/SDS system is shown in Fig. 10.

Conclusions

The thermally induced aggregation behavior of P(MEO_2MA_{90}-co-$OEGMA_{10}$) in aqueous solution is studied and the interaction between P(MEO_2MA_{90}-co-$OEGMA_{10}$) and SDS or DTAB in aqueous solutions with and without salt is explored by using DLS, pyrene fluorescence spectroscopy, and 2D NOESY NMR technology. The influence rule of surfactant on thermo-sensitive behavior of polymer and the corresponding mechanism are revealed. The results have shown that the P(MEO_2MA_{90}-co-$OEGMA_{10}$) has an appreciably reversible thermal responsivity (LCST = 38 °C) in aqueous solution due to a delicate balance between hydrogen bonds between the copolymers and water molecules and hydrophobic interactions of polymer segments. The addition of surfactants changes the aggregation behavior of polymers by interaction with polymers. The self-aggregation of polymer chains is hindered due to the strong electrostatic repulsion and the "locking water" effect caused by surfactant head groups and thus leads to the increase of LCST with the increase of surfactant concentration for the system of polymer/surfactant. When the surfactant concentration is higher than CAC, the aggregation of polymer hydrophobic segments is inhibited completely, and the thermally induced phase transition behavior disappears.

The organic ions Bu_4N^+ and Pr_4N^+ retard the interaction between P(MEO_2MA_{90}-co-$OEGMA_{10}$) and SDS. In P(MEO_2MA_{90}-co-$OEGMA_{10}$)/organic salt/SDS system, the Bu_4N^+-SDS or Pr_4N^+-SDS mixed micelles are formed first, then the mixed micelles bind on the polymer chain forming the polymer-bound Bu_4N^+-SDS or Pr_4N^+-SDS complexes. And the P(MEO_2MA_{90}-co-$OEGMA_{10}$) chain in the P(MEO_2MA_{90}-co-$OEGMA_{10}$)-(Bu_4N^+ or Pr_4N^+-SDS) complex is located only on the complex surface and far away from the surface-attached Bu_4N^+ or Pr_4N^+ ions. Furthermore, the quantitative relations between LCST of different systems and surfactant concentrations were established. The LCST of the system containing P(MEO_2MA_{90}-co-$OEGMA_{10}$) can be adjusted by tailoring the surfactant concentration, salt concentration of the system. The present results not only provide detailed information on the interaction between polymer and

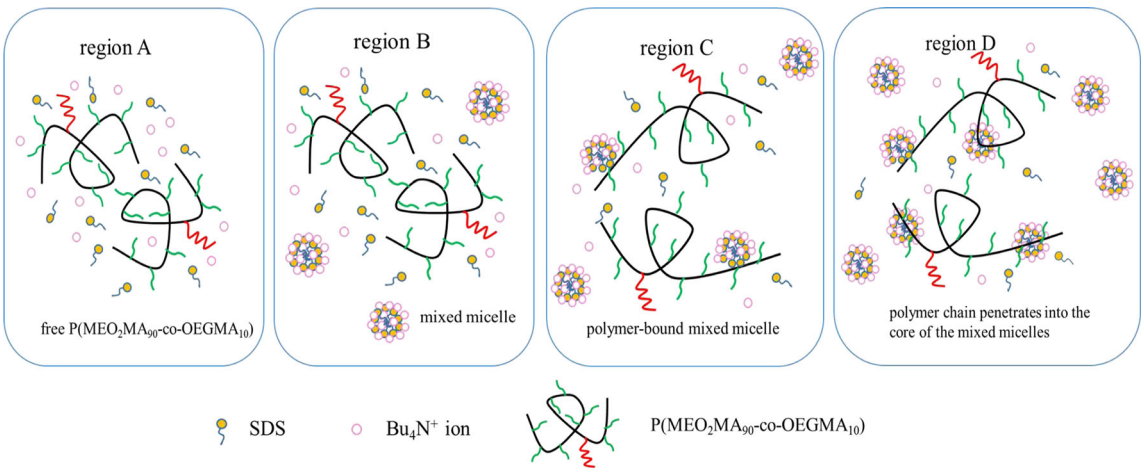

Fig. 10 Schematic illustration of the aggregation process in P(MEO_2MA_{90}-co-$OEGMA_{10}$)/Bu_4NBr/SDS system (C_{Bu4NBr} = 4.4 mM)

ionic surfactants as well as the explicit role of organic salts in influencing the interaction, but also advance our understanding on the general dynamical features and binding mechanism of polymer/ionic surfactant systems.

Acknowledgements This work is supported by the National Natural Science Foundation of China (Projects Nos. 21476072 and 91334203).

Compliance with ethical standards

Conflict of interest The authors declare that they have no conflict of interest.

References

1. Li GZ, JH M, Li Y, Yuan SL (2000) An experimental study on alkaline/surfactant/polymer flooding systems using nature mixed carboxylate. Colloids and Surfaces A: Physicochem Eng Aspects 173:219–229
2. Malmsten M (2002) Surfactants and polymers in drug delivery. Marcel Dekker, New York
3. Penfold J, Taylor DJF, Thomas RK, Tucker I, Thompson LJ (2003) Adsorption of polymer/surfactant mixtures at the Air–Water Interface: Ethoxylated poly(ethyleneimine) and sodium dodecyl sulfate. Langmuir 19:7740–7745
4. Shang BZ, Wang Z, Larson RG (2008) Molecular dynamics simulation of interactions between a sodium dodecyl sulfate micelle and a poly(ethylene oxide) polymer. J Phys Chem B 112:2888–2900
5. Tadros TF (2006) Applied surfactants: principles and applications. Wiley, Weinheim
6. George J, Sudheesh P, Reddy PN, Sreejith L (2009) Influence of salt on cationic surfactant-biopolymer interactions in aqueous media. J Solut Chem 38:373–381
7. La Mesa C (2005) Polymer–surfactant and protein–surfactant interactions. J Colloid Interface Sci 286:148–157
8. Tabor RF, Eastoe J, Dowding PJ (2010) A two-step model for surfactant adsorption at solid surfaces. J Colloid Interface Sci 346: 424–428
9. Tam KC, Wyn-Jones E (2006) Insights on polymer surfactant complex structures during the binding of surfactants to polymers as measured by equilibrium and structural techniques. Chem Soc Rev 35:693–709
10. Gjerde MI, Nerdal W, Høiland H (1996) A NOESY NMR study of the interaction between sodium dodecyl sulfate and poly(ethylene oxide). J Colloid Interface Sci 183:285–288
11. Hou SS, Tzeng JK, Chuang MH (2010) Intermolecular association and supramolecular structures of PNVF-LiPFN and PVP-LiPFN complexes in the aqueous phase. Soft Matter 6:409–415
12. Landry J, Marangoni DG, Arden D, MacLennan I, Kwak JT (2009) A 1D- and 2D-NMR study of an anionic surfactant/neutral polymer complex. J Surfact Deterg 12:155–164
13. Lin JH, Hou SS (2014) Effects of organic salts on polymer–surfactant interactions: roles of Bu_4NBr and Pr_4NBr in PVP–SDS complexation. Macromolecules 47:6418–6429
14. Tzeng JK, Hou SS (2008) Interactions between poly(N-vinylformamide) and sodium dodecyl sulfate as studied by fluorescence and two-dimensional NOE NMR spectroscopy. Macromolecules 41:1281–1288
15. Dai S, Tam KC, Li L (2001) Isothermal titration calorimetric studies on interactions of ionic surfactant and poly(oxypropylene)−Poly(oxyethylene)−Poly(oxypropylene) triblock copolymers in aqueous solutions. Macromolecules 34: 7049–7055
16. Banipal T, Kaur H, Banipal P, Sood A (2014) Effect of head groups, temperature, and polymer concentration on surfactant–polymer interactions. J Surfact Deterg 17:1181–1191
17. Benrraou M, Bales B, Zana R (2003) Effect of the nature of the counterion on the interaction between cesium and tetraalkylammonium dodecylsulfates and poly(ethylene oxide) or poly(vinylpyrolidone). J Colloid Interface Sci 267:519–523
18. Chauhan S, Singh R, Sharma K, Kumar K (2015) Interaction study of anionic surfactant with aqueous non-ionic polymers from conductivity, density and speed of sound measurements. J Surfact Deterg 18:225–232
19. Wang R, Wang Y (2013) Interaction of anionic sulfonate Gemini surfactant with PEO-PPO-PEO triblock copolymers. Acta Chim Sin 72:41–50
20. Chakraborty T, Chakraborty I, Ghosh S (2006) Sodium carboxymethylcellulose-CTAB interaction: a detailed thermodynamic study of polymer-surfactant interaction with opposite charges. Langmuir 22:9905–9913
21. Fegyver E, Mészáros R (2014) The impact of nonionic surfactant additives on the nonequilibrium association between oppositely charged polyelectrolytes and ionic surfactants. Soft Matter 10: 1953–1962
22. Fegyver E, Mészáros R (2015) Complexation between sodium poly (styrenesulfonate) and Alkyltrimethylammonium bromides in the presence of dodecyl maltoside. J Phys Chem B 119:5336–5346
23. Li D, Kelkar MS, Wagner NJ (2012) Phase behavior and molecular thermodynamics of coacervation in oppositely charged polyelectrolyte/surfactant systems: a cationic polymer JR 400 and anionic surfactant SDS mixture. Langmuir 28:10348–10362
24. Dai S, Tam KC, Jenkins RD (2001) Binding characteristics of hydrophobic ethoxylated urethane (HEUR) and an anionic surfactant: Microcalorimetry and laser light scattering studies. J Phys Chem B 105:10189–10196
25. Niranjan PS, Shukla R, Upadhyay S (2012) Interactions of polyacrylamide with cationic surfactants: thermodynamic and surface parameters. J Surfact Deterg 15:53–57
26. Öztekin N, Erim FB (2013) Determination of critical aggregation concentration in the poly-(vinylpyrrolidone)–sodium dodecyl sulfate system by capillary electrophoresis. J Surfact Deterg 16:363–367
27. Dan A, Ghosh S, Moulik SP (2008) The solution behavior of poly(-vinylpyrrolidone): its clouding in salt solution, solvation by water and isopropanol, and interaction with sodium dodecyl sulfate. J Phys Chem B 112:3617–3624
28. Karlstroem G, Carlsson A, Lindman B (1990) Phase diagrams of nonionic polymer-water systems: experimental and theoretical studies of the effects of surfactants and other cosolutes. J Phys Chem 94: 5005–5015
29. Majhi PR, Moulik SP, Burke SE, Rodgers M, Palepu R (2001) Physicochemical investigations on the interaction of surfactants and salts with polyvinylpyrrolidone in aqueous medium. J Colloid Interface Sci 235:227–234
30. Maltesh C, Somasundaran P (1992) Effect of binding of cations to polyethylene glycol on its interactions with sodium dodecyl sulfate. Langmuir 8:1926–1930
31. Norwood DP, Minatti E, Reed WF (1998) Surfactant/polymer assemblies. 1. Surfactant binding properties. Macromolecules 31: 2957–2965
32. Sorci GA, Reed WF (2002) Electrostatic and association phenomena in aggregates of polymers and micelles. Langmuir 18:353–364

33. Xia J, Dubin PL, Kim Y (1992) Complex formation between poly(oxyethylene) and sodium dodecyl sulfate micelles: light scattering, electrophoresis, and dialysis equilibrium studies. J Phys Chem 96:6805–6811
34. Guo Y, Liu HJ, Chen JQ, Shang YZ, Liu HL (2015) Synthesis of P(MEO_2MA-co-OEGMA) random copolymers and thermally induced phase transition behaviors in aqueous solutions. Acta Phys - Chim Sin 31:1914–1923
35. Lutz J-F, Hoth A (2006) Preparation of ideal PEG analogues with a tunable Thermosensitivity by controlled radical copolymerization of 2-(2-methoxyethoxy)ethyl methacrylate and oligo(ethylene glycol) methacrylate. Macromolecules 39:893–896
36. Lin JH, Chen WS, Hou SS (2013) NMR studies on effects of tetraalkylammonium bromides on micellization of sodium dodecylsulfate. J Phys Chem B 117:12076–12085
37. Turro NJ, Baretz BH, Kuo PL (1984) Photoluminescence probes for the investigation of interactions between sodium dodecylsulfate and water-soluble polymers. Macromolecules 17:1321–1324
38. Penfold J, Thomas RK, DJF T (2006) Polyelectrolyte/surfactant mixtures at the air–solution interface. Curr Opin Colloid Interface Sci 11:337–344
39. Taylor DJF, Thomas RK, Penfold J (2007) Polymer/surfactant interactions at the air/water interface. Adv Colloid Interf Sci 132:69–110
40. Kuo PL, Hou SS, Teng CK, Liang WJ (2001) Function and performance of silicone copolymer (VI). Synthesis and novel solution behavior of water-soluble polysiloxanes with different hydrophiles. Colloid Polym Sci 279:286–291
41. Shannigrahi M, Bagchi S (2005) Influence of a neutral polymer (PVP) on the solvatochromic properties of SDS micelles. J Phys Chem B 109:14567–14572
42. Roscigno P, Asaro F, Pellizer G, Ortona O, Paduano L (2003) Complex formation between poly(vinylpyrrolidone) and sodium Decyl sulfate studied through NMR. Langmuir 19:9638–9644